The Astrophysical Journal Letters, 878:L21 (6pp), 2019 June 10 https://doi.org/10.3847/2041-8213/ab2599

Survey of Li-rich Giants among *Kepler* and LAMOST Fields: Determination of Li-rich Giants' Evolutionary Phase

Raghubar Singh[1,2], Bacham E. Reddy[1], Yerra Bharat Kumar[3,5], and H. M. Antia[4]
[1] Indian Institute of Astrophysics 560034, 100ft road Koramangala, Bangalore, India; raghubar2015@gmail.com, raghubar.singh@iiap.res.in
[2] Pondicherry University R. V. Nagara, Kala Pet, 605014, Puducherry, India
[3] Key Laboratory for Optical Astronomy, National Astronomical Observatories, Chinese Academy of Sciences, Beijing, 100101, People's Republic of China
[4] Tata Institute of Fundamental Research Mumbai, India
Received 2019 May 15; revised 2019 May 30; accepted 2019 May 30; published 2019 June 11

Abstract

In this Letter, we report the discovery of 24 new super Li-rich ($A(\mathrm{Li}) \geqslant 3.2$) giants of He-core burning phase at the red clump region. Results are based on a systematic search of a large sample of about 12,500 giants common to the LAMOST spectroscopic and Kepler time-resolved photometric surveys. The two key parameters derived from *Kepler* data are an average period spacing (Δp) between $l = 1$ mixed gravity-dominated g-modes and average large frequency-separation ($\Delta\nu$) $l = 0$ acoustic p-modes, which suggest all the Li-rich giants are in the He-core burning phase. This is the first unbiased survey subjected to a robust technique of asteroseismic analysis to unambiguously determine the evolutionary phase of Li-rich giants. The results provide strong evidence that the Li enhancement phenomenon is associated with giants in the He-core burning phase post He-flash, rather than any other phase on the red giant branch with an inert He-core surrounded by a H-burning shell.

Key words: asteroseismology – stars: abundances – stars: evolution – stars: late-type – stars: low-mass

1. Introduction

It is firmly established that Li-rich giants do exist, though they are not very common (they comprise ~1% of red giants). Thanks to recent large surveys such as LAMOST (Cui et al. 2012) and GALAH (De Silva et al. 2015) there are now a few hundred Li-rich giants that have a Li abundance of $A(\mathrm{Li}) \geqslant 1.5$ dex,[6] a commonly adopted upper limit for normal giants of the red giant branch (RGB; Iben 1967). For example, a recent large study by Deepak & Reddy (2019) discovered more than 300 Li-rich giants from the GALAH spectroscopic survey, doubling the number of Li-rich giants known until then since their first discovery by Wallerstein & Sneden (1982). However, there is no consensus on the origin of Li excess in red giants, which has been elusive for decades. This is because there is no clarity regarding their evolutionary phase, a key parameter for identifying the source of Li enhancement.

Presently, the evolutionary phase of most Li-rich giants is based on their location in the T_{eff}–L plane of the Hertzsprung–Russell (HR) diagram. This source is fraught with ambiguity, as uncertainties in derived stellar parameters arising from different methodologies by different studies are often larger than the differences in stellar parameters of T_{eff} and L between different locations on the HR diagram. As a result, different studies have suggested different phases for Li-rich giants: below the luminosity bump (e.g., Casey et al. 2016), at the bump (e.g., Charbonnel & Balachandran 2000), the red clump (e.g., Kumar et al. 2011; Silva Aguirre et al. 2014; Monaco et al. 2014; Singh et al. 2019), and anywhere along the RGB (e.g., Lebzelter et al. 2012; Martell & Shetrone 2013). These results led to suggestions of different scenarios for the origin of Li excess in red giants: e.g., diffusion of Li upward (in the case of sub-giants), some kind of extra mixing associated with the luminosity bump (e.g., Palacios et al. 2001), nucleosynthesis and dredge-up during the He-flash in the case of a red clump (Kumar et al. 2011), and external scenarios such as mergers of planet or sub-stellar objects for the occurrence of Li-rich giants anywhere along the RGB (Lebzelter et al. 2012). It is important to address the question of whether the Li-rich phenomenon is confined to a single evolutionary phase or to multiple phases on the RGB. For this to be answered an independent method is needed.

Asteroseismic analysis is one of the robust methods for separating giants ascending the RGB with a He-inert core from those with core He-burning (Bedding et al. 2011) red clump giants, post He-flash. *Kepler* (Borucki et al. 2010) time-resolved photometric data can be used for this purpose. Unfortunately, none of the known Li-rich giants are in the *Kepler* fields, barring a few recently reported ones. To date, there are only six Li-rich giants that were analyzed using *Kepler* and *CoRoT* asteroseismic data. With the exemption of one (Jofré et al. 2015), all five giants have been found to be He-core burning giants of a red clump (Silva Aguirre et al. 2014; Carlberg et al. 2015; Bharat Kumar et al. 2018; Smiljanic et al. 2018). It is necessary to conduct a large unbiased systematic survey of Li-rich giants that have asteroseismic data. In this Letter, we show results from the survey based on large red giant sample stars of about 12,500 that are common among LAMOST spectroscopic and *Kepler* photometric surveys.

2. Sample Selection

The primary purpose of this study is to accurately and unambiguously determine the evolutionary phase of Li-rich giants. For this we adopted sample giants that are common among the *Kepler* (KIC; Mathur et al. 2017) and LAMOST spectroscopic catalogs. By applying the criteria $\log g \leqslant 3.5$ and $T_{\mathrm{eff}} \leqslant 5500$ K for RGB giants, we found a sample of 23,000 giants in the *Kepler* Input Catalog. Of these, about 12,500 giants are found to be common in the LAMOST catalog of data

[5] LAMOST Fellow.
[6] $A(\mathrm{Li}) = \log 10(N(\mathrm{Li})/N(\mathrm{H})) + 12$.

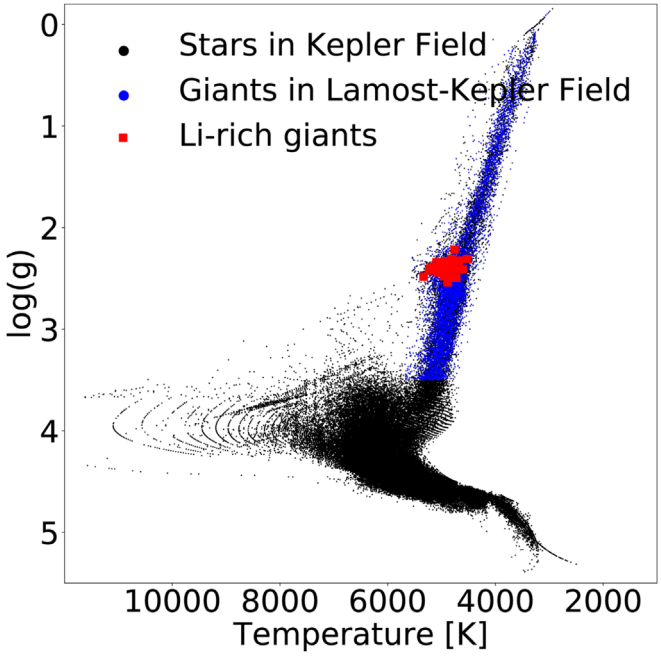

Figure 1. Survey sample of 12,500 giants (blue symbols), along with the entire sample from the *Kepler* catalog as background (black symbols). The red symbols represent giants with a strong Li line at 6707 Å.

release 4 (DR4).[7] LAMOST is a low-resolution ($R = 1800$) spectroscopic survey of stars covering a wavelength range of 3700–9000 Å. Continuum-fitted spectra have been inspected for the presence of a Li resonance line at 6707 Å and 78 spectra were found to have strong Li line. The common sample of giants among *Kepler* and LAMOST (blue dots), along with the entire sample from the *Kepler* catalog (Mathur et al. 2017) as background (black dots), are shown in Figure 1. Stars that feature a strong Li line at 6707 Å are shown as red squares. Note that all of them are concentrated in a particular range of $\log g$, which coincides with the positions of both a red clump and a luminosity bump in the HR diagram.

3. Lithium Abundance

Spectra of Li-rich giants with a strong Li resonance line at 6707 Å are shown in Figure 2 along with the known Li-rich giant KIC 12645107 on the top and a normal Li giant at the bottom. For estimating Li abundance from low-resolution spectra we used a method that was successfully demonstrated previously by Kumar et al. (2011, 2018). This method involves measuring the Li line strength at 6707 Å relative to an adjacent Ca I line at 6717 Å; both are zero low-excitation potential lines and show similar sensitivity to $T_{\rm eff}$. The derived ratios of Li 6707 Å core strength to Ca 6717 Å are plugged into correlations between Li abundance and line strength ratios derived by Kumar et al. (2018). Because uncertainties are relatively higher, 0.3–0.4 dex, the sample has been restricted to only giants with a very strong Li line or the estimated Li abundance $A(\rm Li) \geqslant 3.0$ dex. This is to avoid mistaking normal giants with $A(\rm Li) \leqslant 1.8$ dex (Iben 1967). We found 26 giants with $A(\rm Li) \geqslant 3.0$ dex and half a dozen have A (Li) $\geqslant 4.0$ dex, which is about an order of magnitude more than the current ISM value (3.3 dex), and about a factor of 100 more than the

[7] http://dr4.lamost.org/

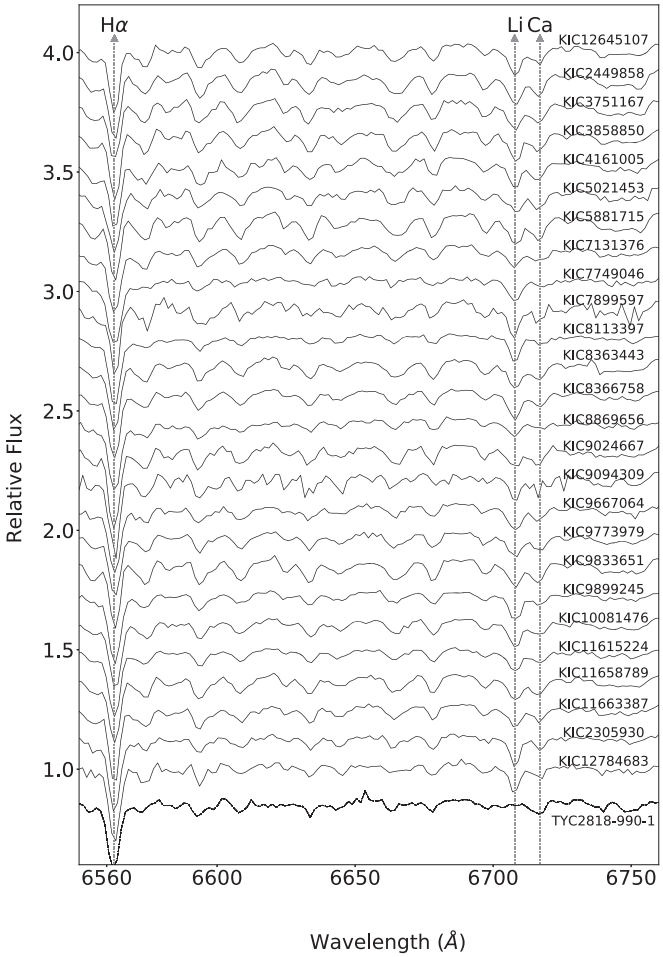

Figure 2. Spectra of 26 Li-rich giants showing an exceptionally strong Li resonance line at 6707 Å. Also shown are the two reference spectra of known super Li-rich giants (KIC 12645107, KIC 2305930) with A(Li) = 3.3, 4.1 dex and a normal Li giant of A(Li) = 0.5 dex (bottom, TYC 2818-990-1).

maximum predicted abundance of A(Li) = 1.8 dex (Iben 1967). Estimated Li abundances, along with [Fe/H], $T_{\rm eff}$, and log g (stellar parameters from the LAMOST DR4 catalogs), are given in Table 1. Two of these have been recently reported as Li-rich giants (Bharat Kumar et al. 2018) based on high-resolution spectra. The mean difference between the estimated A(Li) in this study and the literature values based on high-resolution spectra is 0.2 dex, which agrees well within the uncertainties.

4. Analysis of Asteroseismic Data

All 26 Li-rich giants that are given in Table 1 have long cadences (29.4 minutes) of 10–17 quarters of *Kepler* photometric data. It is known that red giants show oscillations of mixed modes of gravity (g-mode) arising from the central core and acoustics modes (p-modes) arising in the convective envelope (De Ridder et al. 2009; Beck et al. 2011). In this work we have used the lightkurve package (https://github.com/KeplerGO/lightkurve) for merging individual quarters into a combined light curve, and converting the combined light curve into a power density spectrum (PDS) using the Lomb–Scargle Fourier transform. In Figure 3(a), the PDS for one of the sample stars of KIC 11615224 from Table 1 is given, and its solid line is the fitting for the background. A background-

Table 1
List of Li-rich Giants

KIC (1)	Vmag (2)	A(Li)[a] (3)	ΔP (4)	A(Li) (5)	ν_{max} (6)	$\Delta\nu$ (7)	T_{eff} (8)	Mass (9)	Radius (10)	log g (11)	[Fe/H] (12)	M[b] (13)
2305930	11.02	4.20	226	4.1	27.2	4.0	4861 ± 40	0.71 ± 0.1	9.40 ± 0.7	2.40 ± 0.1	−0.50 ± 0.0	2
2449858	13.38	⋯	235	3.3	26.8	3.5	4840 ± 30	1.15 ± 0.1	12.1 ± 0.5	2.50 ± 0.1	−0.15 ± 0.0	1
3751167	13.83	⋯	419	4.0	26.1	3.6	4777 ± 239	0.91 ± 0.2	10.9 ± 1.0	2.25 ± 0.4	−1.06 ± 0.2	2
3858850	12.44	⋯	192	3.3	25.9	3.5	4434 ± 50	0.90 ± 0.1	11.1 ± 0.6	2.62 ± 0.1	0.27 ± 0.1	1
4161005	13.93	⋯	247	3.3	29.1	3.9	4897 ± 40	0.93 ± 0.2	10.7 ± 0.8	2.35 ± 0.1	−0.52 ± 0.0	1
5021453	11.25	⋯	314	4.0	31.8	4.0	4754 ± 26	1.02 ± 0.1	10.5 ± 0.6	2.55 ± 0.1	−0.08 ± 0.0	1
5881715	11.64	⋯	191	3.8	30.9	3.4	4786 ± 35	1.85 ± 0.2	14.2 ± 0.7	2.35 ± 0.1	−0.15 ± 0.0	1
7131376	13.99	⋯	190	3.8	34.8	4.1	4696 ± 80	1.18 ± 0.1	10.8 ± 0.4	2.68 ± 0.1	0.08 ± 0.1	1
7749046	13.47	⋯	235	4.2	29.9	3.8	4891 ± 26	1.13 ± 0.1	11.2 ± 0.4	2.36 ± 0.1	−0.71 ± 0.0	3
7899597	13.61	⋯	224	3.9	31.6	3.8	4710 ± 50	1.26 ± 0.2	11.7 ± 0.9	2.49 ± 0.1	−0.10 ± 0.1	1
8113379	13.13	⋯	273	3.2	31.2	3.9	4757 ± 40	1.06 ± 0.1	10.7 ± 0.4	2.53 ± 0.1	−0.06 ± 0.0	1
8363443	10.95	⋯	217	3.5	32.4	3.8	4490 ± 40	1.28 ± 0.1	11.8 ± 0.3	2.58 ± 0.1	0.23 ± 0.0	1
8366758	12.50	⋯	218	3.8	26.4	3.9	4664 ± 50	0.67 ± 0.1	9.3 ± 0.3	2.57 ± 0.1	0.18 ± 0.0	1
8869656	9.34	⋯	240	4.1	30.7	3.8	4764 ± 30	1.15 ± 0.1	11.3 ± 0.5	2.44 ± 0.1	−0.30 ± 0.0	1
9024667	12.28	⋯	449	3.4	25.2	3.5	4555 ± 35	0.83 ± 0.1	10.7 ± 0.7	2.59 ± 0.1	0.16 ± 0.0	1
9094309	14.31	⋯	253	4.0	33.2	4.1	4919 ± 129	1.16 ± 0.1	10.8 ± 0.5	2.55 ± 0.2	−0.32 ± 0.1	2
9667064	13.35	⋯	176	4.4	30.2	3.6	4678 ± 211	1.34 ± 0.2	12.4 ± 0.7	2.28 ± 0.3	−0.10 ± 0.2	1
9773979	14.30	⋯	487	3.2	32.6	4.0	4622 ± 86	1.15 ± 0.2	11.0 ± 0.6	2.48 ± 0.1	−0.05 ± 0.1	2
9833651	12.52	⋯	174	3.6	38.8	4.2	4683 ± 44	1.47 ± 0.1	11.4 ± 0.4	2.67 ± 0.1	0.09 ± 0.0	1
9899245	13.04	⋯	150	3.4	33.2	3.9	4700 ± 30	1.30 ± 0.3	11.6 ± 0.8	2.72 ± 0.1	0.10 ± 0.0	1
10081476	13.84	⋯	211	3.8	26.6	3.4	4453 ± 50	1.07 ± 0.2	11.9 ± 0.8	2.52 ± 0.1	0.24 ± 0.0	1
11615224	11.16	⋯	257	3.3	30.0	4.0	4746 ± 25	0.85 ± 0.1	9.80 ± 0.4	2.40 ± 0.1	−0.04 ± 0.02	2
11658789	13.36	⋯	228	3.9	31.2	4.3	4999 ± 75	0.81 ± 0.1	9.30 ± 0.6	2.48 ± 0.1	−0.70 ± 0.1	2
11663387	12.59	⋯	217	4.0	32.7	4.1	4642 ± 40	1.01 ± 0.1	10.4 ± 0.2	2.49 ± 0.1	0.02 ± 0.0	1
12645107	11.40	3.24	243	3.5	30.4	3.8	4853 ± 40	1.14 ± 0.1	11.2 ± 0.4	2.39 ± 0.1	−0.22 ± 0.0	1
12784683	11.10	⋯	239	3.4	28.7	3.7	4862 ± 25	1.11 ± 0.2	11.4 ± 0.7	2.33 ± 0.1	−0.28 ± 0.0	1

Notes. Yu et al. (2018) also classifies these stars as red clumps.
[a] Li abundance of two stars from Bharat Kumar et al. (2018).
[b] Milky way membership: 1: thin disk; 2: thick disk; 3: halo star.

subtracted and smoothed PDS (Figure 3(b)) is used to identify modes and measure their frequencies.

There are two key parameters: frequency separation between two consecutive radial ($l = 0$) modes ($\Delta\nu$) and period separation between two consecutive dipole ($l = 1$) modes (Δp), which are used to separate the red giants of the He-burning core of the red clump and the He-inert core of the RGB (Bedding et al. 2011). From the smoothed PDS radial modes $l = 0$, dipole modes ($l = 1$) and quadruple modes ($l = 2$) have been identified and the corresponding frequencies for 4–5 modes ($l = 0$) in the PDS of each star are measured. The values of $\Delta\nu$ are those for which modulo or the remainder of $\nu/\Delta\nu$ is the same for the frequencies of the respective measured mode. In Figure 3(c), this has been illustrated for a typical giant, KIC 1165224. For its modes of $l = 0$, $l = 2$, and $l = 1$, we found a value of $\Delta\nu = 4.01\ \mu$Hz, for which modulo is the same for all the frequencies. The values of derived large frequency separation, $\Delta\nu$, are given in Table 1. After measuring the frequency corresponding to detected dipole modes ($l = 1$, g-modes), we calculate the period of dipole modes and period spacing between the consecutive dipole modes, which are given in Figure 3(d). The median value of derived period spacing is considered the gravity mode period spacing of a star (Stello et al. 2013). The derived values of $\Delta\nu$ and Δp, given in Table 1, suggest all the Li-rich giants are He-core burning red clump stars. Our analysis agrees well with the recent study done by Yu et al. (2018). The average differences between our study and Yu et al. (2018) for $\Delta\nu$ and ν_{max} are 0.8 and 0.1 μHz, respectively.

Stellar parameters such as radius and mass have been derived using the seismic parameters and the calibrations are given by Kjeldsen & Bedding (1995). All the giants have low mass, with $M \leqslant 2.0\,M_{\odot}$ (Table 1). Furthermore, light curves show no indication of major flaring activity, which is in agreement with a lack of visible asymmetry or emission profiles of H_{α} in the spectra (Figure 2), indicating no significant stellar activity in the photospheres of the stars.

5. Discussion

This is the first survey of its kind to be based on a large unbiased sample survey of giants that are common among LAMOST spectroscopic and *Kepler* photometric surveys. Analysis yielded a total of 26 Li-rich giants. Abundance results and the derived asteroseismic parameters, $\Delta\nu$ and Δp, are given in Table 1, and are shown in the plot of Δp and $\Delta\nu$ (Figure 4). Known RC and RGB giants based on asteroseismic analysis form the background. As shown in Figure 4, all the Li-rich giants from this study show large values of $\Delta p \geqslant 150$ s and small values of $\Delta\nu \leqslant 5\ \mu$Hz, and occupy the He-core burning phase region of the $\Delta\nu - \Delta p$ diagram (Bedding et al. 2011). Interestingly, none of the Li-rich giants found in this survey are on the ascending RGB. The results imply that the Li enhancement phenomenon is probably associated with the He-flash at the tip of the RGB or post He-flash rather than on the RGB.

As earlier stated, there are only six Li-rich giants for which the evolutionary phase is determined based on asteroseismology. All of them were discovered serendipitously. Of these five

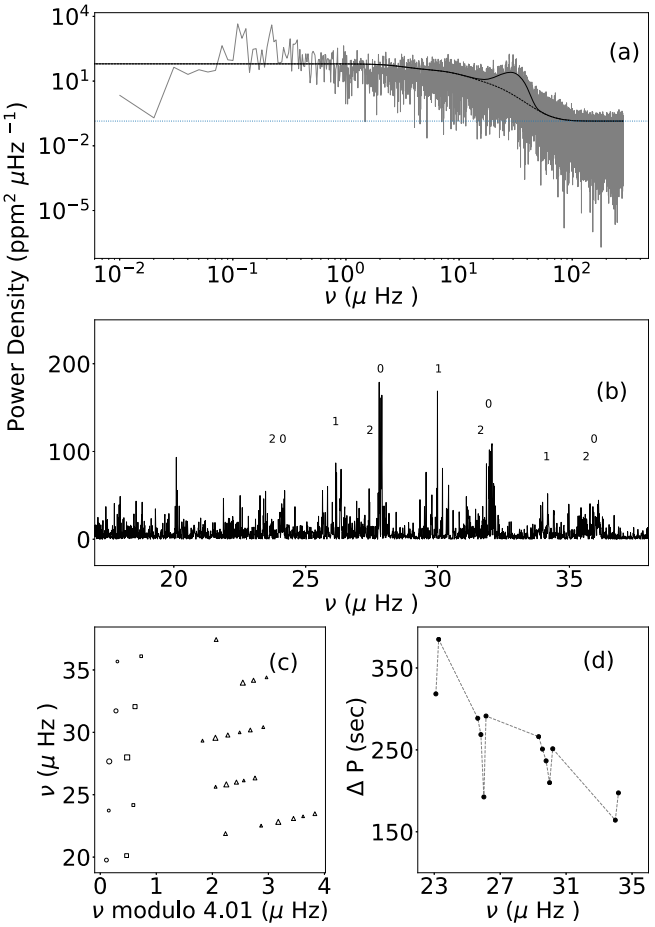

Figure 3. Top panel: the gray region in the background is the PDS of KIC 11615224 and the solid black line is the global background fit to the PDS. Middle panel: $l = 0$, 1, 2 modes in the PDS. Bottom panel: measurement of the large frequency separation and gravity mode period spacing of star. In the bottom left panel the circles are modes corresponding to $l = 0$, the squares are modes corresponding to $l = 2$, and the triangles are modes corresponding to $l = 1$.

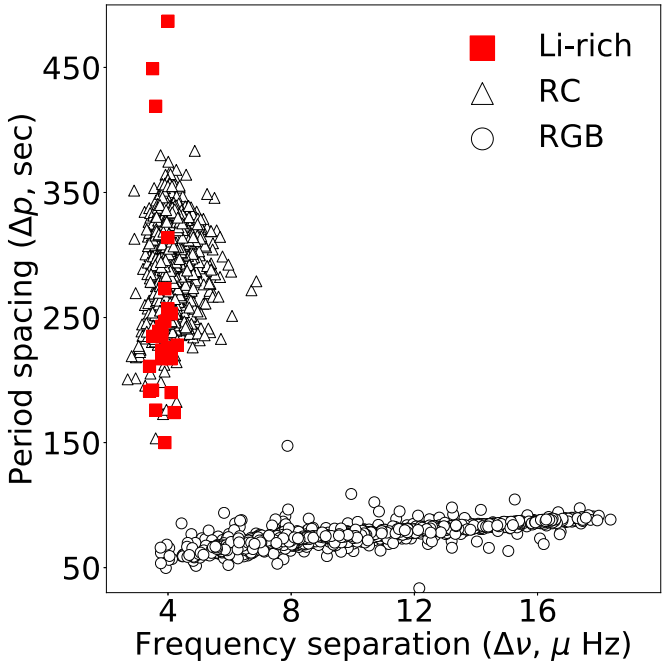

Figure 4. Li-rich giants discovered in this study (red squares) shown in a $\Delta\nu$–Δp asteroseismic diagram. Giants classified based on asteroseismic analysis form the background: He-core burning RC giants (open triangle) and inert He-core giants ascending the RGB for the first time (open circle). Note that all the Li-rich giants are on the RC region of the diagram.

are unambiguously classified as giants of the He-core burning phase in the red clump region (Silva Aguirre et al. 2014; Carlberg et al. 2015; Bharat Kumar et al. 2018; Smiljanic et al. 2018) and one as RGB near the bump(Jofré et al. 2015). The lone exception is KIC 9821622 (Jofré et al. 2015). Though this is a bona fide RGB star with an inert He-core and H-burning shell ($\Delta\nu = 6.07$ μHz and $\Delta p = 67.6$ s), its categorization as a Li-rich giant is not beyond doubt, as the Li abundance (LTE: A (Li) $= 1.49$ dex and NLTE: 1.65 dex) measured from a well-defined and much stronger line at 6707 Å is at the border line. It is important to establish whether this particular star is indeed a Li-rich giant, as it has serious implications for identifying the source of Li enrichment in red giants.

Of course, there are many Li-rich giants in the literature that have been reported as being on the RGB based on their positions in the HR diagram. This method is found to be uncertain for determining exact evolutionary phase. For example, of the five asteroseismically known Li-rich RC giants, KIC 4937011 was initially reported as an RGB star below the bump by Anthony-Twarog et al. (2013) and Carlberg et al. (2015) based on its location in the HR diagram. However, its derived asteroseismic parameters, $\Delta\nu = 4.15$ μHz and $\Delta p = 249.9$ s (Vrard et al. 2016), firmly put the giant in the He-core burning phase. This illustrates the difficulty of determining their precise evolutionary phase. We also note another recent study by Yan et al. (2018) in which they reported TYC 429-2097-1 as the most Li-rich giant, with A (Li) $= 4.51$ dex, and located it at the bump based on its location in the HR diagram. This star is not in the *Kepler* field. However, its derived ratio of [C/N] $= -0.47 \pm 0.10$ is more compatible with it being in the red clump (Hawkins et al. 2016; Singh et al. 2019). In fact, Casey et al. (2016) made an important observation that although the stellar parameters of the majority of Li-rich giants are consistent with being on the RGB at or below the luminosity bump, they are each individually consistent with being RC. However, they could not conclude that they are indeed RC giants based on available data to them. Does this mean that a number of Li-rich giants that are reported to be on the RGB based on L and $T_{\rm eff}$ are misclassified? The results of this study seem to suggest that this is a real possibility.

Due to ambiguity in the Li-rich giants' evolutionary phase, numerous models have been constructed to explain Li excess using the prevailing conditions at each of the suggested multiple phases on the RGB. Broadly, theoretical models fall into two categories: external and in situ scenarios. One of the external scenarios is the merger of planets or sub-stellar objects such as brown dwarfs. This is invoked with the expectation that planets or brown dwarfs contain reservoirs of primordial Li with little or no depletion, and their mergers will enhance the photospheric Li abundance of a star either by direct addition of the Li reservoir to the photosphere or by induced mixing due to angular momentum transfer to the star or a combination of both (see, e.g., Siess & Livio 1999; Casey et al. 2016). This scenario gained merit with evidence that large planets in close-in orbits are less frequent among sub-giants compared to their main-sequence counterparts (Villaver et al. 2014).

However, to account for the levels of Li seen in many of the super Li-rich giants would require mergers of several Jupiter-size planets with undiluted Li reservoirs (Carlberg et al. 2012). The merger of such large numbers of planets is very unlikely. Also, theoretical models put a maximum limit on Li abundance due to such mergers at $A(\mathrm{Li}) = 2.2$ dex (Aguilera-Gómez et al. 2016). Furthermore, contrary to our results, an engulfment scenario suggests the occurrence of Li-rich giants anywhere along the RGB and the presence of infrared excess as a result of merger impact. Our results support the argument by Deepak & Reddy (2019) against an external scenario, based on the frequency of Li-rich giants occurring at various phases. They show that, disproportionately, large numbers of Li-rich giants belong to the red clump compared to any other phase on the RGB.

The second scenario is the in situ origin, which entails Li production via the Cameron & Fowler mechanism (Cameron & Fowler 1971), $^3\mathrm{He}(\alpha, \gamma)^7\mathrm{Be}(e^-, \nu)^7$ Li. In the case of Li enhancement in the photospheres of highly evolved massive ($\geqslant 3 - 4M_{\odot}$) asymptotic giants branch stars (Smith & Lambert 1989) this mechanism is expected to operate just below the convective envelope, which is hot enough to produce ^{7}Be and close enough for ^{7} Be to get transported to cooler upper layers where it can form ^{7}Li. This process is known as hot bottom burning. In the case of low-mass RGB giants convection between the H-burning shell and the outer convective layers is inhibited by the radiative zone, and standard models (Iben 1967) do not predict changes in abundances after the first dredge-up. However, observations of giants after the first dredge-up do show severe depletion of Li and reduction in the 12C/13C ratios (Gilroy & Brown 1991) compared to standard models of the first dredge-up on RGB Iben (1967). For example, severe depletion of Li starting from the bump has been illustrated for giants in globular cluster NGC 6397 by Lind et al. (2009). These anomalies were explained by extra mixing at the luminosity bump at which the barrier for the deep mixing is erased (see, e.g., Eggleton et al. 2008). Ironically, a bump has also been suggested as a source of Li enhancement (Palacios et al. 2001; Charbonnel 2005; Denissenkov et al. 2009), as many early observations showed Li-rich giants coinciding with the bump in the HR diagram (Charbonnel & Balachandran 2000; Kumar & Reddy 2009). It would be a challenging task to explain Li enhancement at the same phase where severe Li depletion is known to occur. Even if we assume a bump as the origin of Li excess, it is unlikely Li can survive through the deep convection phase from the bump to the clump, and importantly, sustain the high levels of Li abundance seen in many of the super Li-rich giants. Given that the Li-rich phase of the RGB is a transient phenomenon lasting for a short period of about 6M years (Palacios et al. 2001) compared to, for example, the 50–100 Myr (see also Deepak & Reddy 2019) evolutionary period from the bump to the RGB tip, it is very unlikely that the high Li abundances seen in these red clump stars originated at the luminosity bump.

6. Conclusion

In this study we addressed the longstanding problem of precisely determining the stellar evolutionary phase of Li-rich giants. Our results are based on a large unbiased sample of 12,500 low-mass RGB giants common among *Kepler* photometric and LAMOST spectroscopic surveys. We found 24 new Li-rich giants with a Li abundance of $A(\mathrm{Li}) \geqslant 3.0$ dex, which is more than an order of magnitude larger than the maximum predicted abundance of $A(\mathrm{Li}) = 1.80$ dex. Importantly, the derived asteroseismic parameters, $\Delta\nu$ and Δp, show that all the Li-rich giants are in the He-core burning phase, and are at the red clump region. This is the most unambiguous evidence so far that the Li enhancement phenomenon is probably associated only with the He-core burning phase rather than being on the RGB with an inert He-core. The He-flash at the tip, the event that immediately precedes a red clump, can be explored to explain the Li excess in red clump giants.

Y.B.K is thankful for the support from NSFC grant No. 11850410437. Funding for LAMOST (www.lamost.org) has been provided by the Chinese NDRC. LAMOST is operated and managed by the National Astronomical Observatories, CAS. We thank the entire *Kepler* team, without whom this work could not have been possible. We also thank the anonymous referee for the constructive suggestions.

References

Aguilera-Gómez, C., Chanamé, J., Pinsonneault, M. H., & Carlberg, J. K. 2016, ApJ, 829, 127
Anthony-Twarog, B. J., Deliyannis, C. P., Rich, E., & Twarog, B. A. 2013, ApJL, 767, L19
Beck, P. G., Bedding, T. R., Mosser, B., et al. 2011, Sci, 332, 205
Bedding, T. R., Mosser, B., Huber, D., et al. 2011, Natur, 471, 608
Bharat Kumar, Y., Singh, R., Eswar Reddy, B., & Zhao, G. 2018, ApJL, 858, L22
Borucki, W. J., Koch, D., Basri, G., et al. 2010, Sci, 327, 977
Cameron, A. G. W., & Fowler, W. A. 1971, ApJ, 164, 111
Carlberg, J. K., Cunha, K., Smith, V. V., & Majewski, S. R. 2012, ApJ, 757, 109
Carlberg, J. K., Smith, V. V., Cunha, K., et al. 2015, ApJ, 802, 7
Casey, A. R., Ruchti, G., Masseron, T., et al. 2016, MNRAS, 461, 3336
Charbonnel, C. 2005, in ASP Conf. Ser. 336, Cosmic Abundances as Records of Stellar Evolution and Nucleosynthesis, ed. T. G. Barnes, III & F. N. Bash (San Francisco, CA: ASP), 119
Charbonnel, C., & Balachandran, S. C. 2000, A&A, 359, 563
Cui, X.-Q., Zhao, Y.-H., Chu, Y.-Q., et al. 2012, RAA, 12, 1197
, Deepak, & Reddy, B. E. 2019, MNRAS, 484, 2000
Denissenkov, P. A., Pinsonneault, M., & MacGregor, K. B. 2009, ApJ, 696, 1823
De Ridder, J., Barban, C., Baudin, F., et al. 2009, Natur, 459, 398
De Silva, G. M., Freeman, K. C., Bland-Hawthorn, J., et al. 2015, MNRAS, 449, 2604
Eggleton, P. P., Dearborn, D. S. P., & Lattanzio, J. C. 2008, ApJ, 677, 581
Gilroy, K. K., & Brown, J. A. 1991, ApJ, 371, 578
Hawkins, K., Masseron, T., Jofré, P., et al. 2016, A&A, 594, A43
Iben, I., Jr. 1967, ApJ, 147, 624
Jofré, E., Petrucci, R., García, L., & Gómez, M. 2015, A&A, 584, L3
Kjeldsen, H., & Bedding, T. R. 1995, A&A, 293, 87
Kumar, Y. B., & Reddy, B. E. 2009, ApJL, 703, L46
Kumar, Y. B., Reddy, B. E., & Lambert, D. L. 2011, ApJL, 730, L12
Kumar, Y. B., Reddy, B. E., & Zhao, G. 2018, JApA, 39, 25
Lebzelter, T., Uttenthaler, S., Busso, M., Schultheis, M., & Aringer, B. 2012, A&A, 538, A36
Lind, K., Primas, F., Charbonnel, C., Grundahl, F., & Asplund, M. 2009, A&A, 503, 545
Martell, S. L., & Shetrone, M. D. 2013, MNRAS, 430, 611
Mathur, S., Huber, D., Batalha, N. M., et al. 2017, ApJS, 229, 30
Monaco, L., Boffin, H. M. J., Bonifacio, P., et al. 2014, A&A, 564, L6
Moshir, M., Kopan, G., Conrow, T., et al. 1990, BAAS, 22, 1325
Mosser, B., Barban, C., Montalbán, J., et al. 2011, A&A, 532, A86
Palacios, A., Charbonnel, C., & Forestini, M. 2001, A&A, 375, L9
Siess, L., & Livio, M. 1999, MNRAS, 308, 1133
Silva Aguirre, V., Ruchti, G. R., Hekker, S., et al. 2014, ApJL, 784, L16
Singh, R., Reddy, B. E., & Kumar, Y. B. 2019, MNRAS, 482, 3822
Skrutskie, M. F., Cutri, R. M., Stiening, R., et al. 2006, AJ, 131, 1163
Smiljanic, R., Franciosini, E., Bragaglia, A., et al. 2018, A&A, 617, A4
Smith, V. V., & Lambert, D. L. 1989, ApJL, 345, L75
Stello, D., Huber, D., Bedding, T. R., et al. 2013, ApJL, 765, L41

Villaver, E., Livio, M., Mustill, A. J., & Siess, L. 2014, ApJ, 794, 3
Vrard, M., Mosser, B., & Samadi, R. 2016, A&A, 588, A87
Wallerstein, G., & Sneden, C. 1982, ApJ, 255, 577
Wright, E. L., Eisenhardt, P. R. M., Mainzer, A. K., et al. 2010, AJ, 140, 1868
Yan, H.-L., Shi, J.-R., Zhou, Y.-T., et al. 2018, NatAs, 2, 790
Yu, J., Huber, D., Bedding, T. R., et al. 2018, ApJS, 236, 42